

1 ***Genome-based targeted sequencing as a reproducible microbial community profiling assay.***

2

3 Jacquelynn Benjamino, Benjamin Leopold, Daniel Phillips[□], and Mark D. Adams*

4

5 The Jackson Laboratory for Genomic Medicine, Farmington, CT

6 [□]Current address: Department of Molecular and Cell Biology, University of Connecticut, Storrs,
7 CT.

8

9 Author Contributions: JB, DP, MDA contributed to the development of experimental design. JB
10 performed sample preparation and data analysis. JB, BL developed probe design pipeline. JB,
11 MDA wrote the manuscript.

12

13 *Corresponding author:

14 The Jackson Laboratory for Genomic Medicine

15 10 Discovery Dr.

16 Farmington, CT 06032

17 mark.adams@jax.org

18

19

20

21 **Abstract**

22 Current sequencing-based methods for profiling microbial communities rely on marker
23 gene (e.g. 16S rRNA) or metagenome shotgun sequencing (mWGS) analysis. We present a new
24 approach based on highly multiplexed oligonucleotide probes designed from reference
25 genomes in a pooled primer-extension reaction during library construction to derive relative
26 abundance data. This approach, termed MA-GenTA: Microbial Abundances from Genome
27 Tagged Analysis, enables quantitative, straightforward, cost-effective microbiome profiling that
28 combines desirable features of both 16S rRNA and mWGS strategies. To test the utility of the
29 MA-GenTA assay, probes were designed for 830 genome sequences representing bacteria
30 present in mouse stool specimens. Comparison of the MA-GenTA data with mWGS data
31 demonstrated excellent correlation down to 0.01% relative abundance and a similar number of
32 organisms detected per sample. Despite the incompleteness of the reference database, NMDS
33 clustering based on the Bray-Curtis dissimilarity metric of sample groups was consistent
34 between MA-GenTA, mWGS and 16S rRNA datasets. MA-GenTA represents a potentially useful
35 new method for microbiome community profiling based on reference genomes.

36

37

38 Main

39 The primary molecular methods for determining microbial composition are based on
40 marker gene sequencing or whole metagenome shotgun sequencing (mWGS). The 16S
41 ribosomal RNA (rRNA) marker gene has been widely used for bacterial profiling for decades
42 across diverse ecosystems^{1,2}. Using this method, taxonomic classification of the bacterial
43 community can be obtained at modest cost and a resolution that ranges from sub-species to
44 family level, depending on the 16S rRNA segment that is sequenced³⁻⁶. Continued reduction in
45 the cost of DNA sequencing has meant that mWGS approaches have become increasingly
46 common due to the greater information on gene content, taxonomic resolution, and strain-
47 level variation⁷, despite higher cost and complexity of data analysis.

48 The Human Microbiome Project⁸ and similar large-scale investments⁹ established
49 methods and reference datasets for characterization of microbial profiles across diverse human
50 body sites. As a result, the tools and reference genome datasets for characterizing human
51 microbiomes are much better developed than for those involving other organisms. The mouse
52 is widely used in microbiome studies that seek to demonstrate a causal role of microbes
53 affecting a given trait and to understand the mechanisms by which microbes contribute to
54 phenotypes¹⁰. The vast majority of mWGS sequences from mouse gut samples have no matches
55 to named organisms in public databases¹¹, substantially limiting the informativeness of this
56 approach.

57 One approach to the limited reference genome sequences is construction of *in silico*
58 genomes based on computational sequence assembly of large mWGS datasets to create
59 “metagenome assembled genomes” or MAGs¹²⁻¹⁴. The integrated Mouse Gut Metagenomic
60 Catalog (iMGMC)¹⁵ is one such effort. Combining 1.3 Tbp of data from 298 mouse metagenomic
61 libraries, Lesker, *et al.* assembled 1.2 million contigs; a subset of these could be grouped into
62 830 high quality MAGs (hqMAGs) that are predicted to be >90% complete and <5%
63 contaminated based on the representation of single copy genes¹⁶.

64 Here we describe a new approach to metagenome profiling termed MA-GenTA
65 (Microbial Abundances from Genome Tagged Analysis) that combines the specificity of mWGS
66 analysis with a simplified laboratory and analytical workflow (Figure 1). The availability of

67 custom-designed highly multiplexed pools of oligonucleotides (“oligos”) has opened
68 possibilities for a range of new assay methods to specifically target microbes at the species,
69 strain, and even gene level. We adapted the Allegro Targeted Genotyping assay’s single primer
70 enrichment technology that is widely used for genotyping^{17,18} and implemented it as a
71 quantitative, straightforward, and cost-effective method for profiling mouse microbial
72 communities based on the iMGMC hqMAGs.

73

74 **Results**

75 The MA-GenTA assay is based on approximating the relative abundance of hundreds of
76 microbial species using sets of probes designed to be unique to each genome. The approach
77 includes design of compatible probes directed at the genomes (or genes) of interest, library
78 construction that uses the probe pools in a primer extension reaction, and integration of data
79 across multiple probes to determine species abundance (Fig. 1). Oligonucleotide probe sets
80 were designed using 830 iMGMC hqMAGs¹⁵. Preliminary results using a padlock probe
81 design^{19,20} suggested that 20 probes per genome were sufficient to provide quantitative relative
82 abundance information (data not shown). The padlock probe assay does not allow decoding of
83 any additional adjacent sequence data for confirmation of probe specificity. We therefore
84 sought to develop a method based on a single-primer extension assay, in which sequence
85 adjacent to each probe is determined, allowing confirmation that the probe did in fact bind to
86 the intended target.

87 Computational analysis suggests that each hqMAG is consistent with representing a
88 single bacterial species and about 12% of hqMAGs are concordant with genome sequences of
89 bacterial isolates that are present in GenBank. Most, though do not correspond with isolated
90 bacteria, so in considering a probe design strategy, we decided to develop two completely
91 independent probe sets for each hqMAG. We reasoned that concordance of relative abundance
92 between these probe sets would provide additional support for the conjecture that the
93 hqMAGs are reasonable approximations of *bona fide* genome sequences and that the
94 organisms they represent are commonly found in the mouse gut.

95 Two defined-composition genomic DNA positive controls and a no-template negative
96 control (NTC) were initially used to assess the specificity of each probe set. *Escherichia coli*
97 gDNA and the ZymoBIOMICS Microbial Community Standard (Mock), which contains three
98 species present in the iMGMC hqMAG set, one of which is an *E. coli* strain, were used as the
99 positive controls.

100 Alignment of primary sequence reads showed that probes from many MAGs were
101 detected for the Allegro and JAX designs for *E. coli* (493, 751), and Mock (264, 315) samples
102 (grey dots in Fig. 2a). The vast majority of the MAGs matched in the *E. coli* and Mock samples
103 were represented by a small number of probes with low relative abundance. After applying a
104 probe-abundance threshold of $\geq 0.001\%$ (Supplementary Fig. 1), there was only 1 MAG
105 represented by >10 probes for both the Allegro and JAX designs in the *E. coli* sample and 3 and
106 2 MAGs for the Allegro and JAX designs in the Mock sample as expected (colored dots in Fig.
107 2a). For the *E. coli* sample, 99.95% and 99.28% of reads mapped to the *E. coli* genome for the
108 Allegro and JAX designs, respectively. For the Mock community sample, 99.92% and 98.36% of
109 reads mapped to the three genomes present in the Allegro design and two in the JAX design,
110 respectively.

111 In negative control samples, only a few thousand reads were obtained. NTC reads
112 corresponded to 179 and 312 different probes and 77 and 138 MAGs in the Allegro and JAX
113 designs, respectively (Fig. 2a). Of these probes, 94 (Allegro) and 142 (JAX) from *E. coli*
114 overlapped with the NTC probes and 66 (Allegro) and 96 (JAX) from the Mock overlapped with
115 the probes in the NTC. There are several potential sources of these reads: 1) contamination of
116 the NTC with mouse stool DNA that was processed on the same batch; 2) contamination of the
117 reagents used for library preparation; 3) self-annealing of primers within the probe set; or 4)
118 sequencing-associated barcode-hopping. While there were many MAGs detected in the NTC,
119 most of those MAGs were represented by only a few probes. No MAGs in the Allegro design
120 and only one MAG in the JAX design had more than 10 probes represented (Fig. 2a). The MAG
121 detected in the JAX dataset (single-China_7-4_110307.52) is a Muribaculaceae and present at
122 high abundance in the majority of mouse samples.

123 The Allegro and JAX probe sets have no sequence overlap, thus they represent two
124 completely independent assays for relative abundance of hqMAGs in mouse specimens. High
125 concordance in probe representation and relative abundance would therefore support both the
126 reliability of the MA-GenTA assay and the structural validity of the detected MAGs as
127 representing a species present in the test sample. The Allegro and JAX probe sets were used to
128 assay 72 mouse stool pellet samples, averaging 3.7 million sequencing reads per sample (Table
129 1, Supplementary Table 1). All reads for both datasets were mapped to the iMGMC hqMAGs
130 reference. After mapping, reads that mapped to multiple regions were removed to produce
131 uniquely mapped reads. The uniquely mapped reads were then filtered to include only reads
132 that aligned adjacent to the designed probe region; this allowed us to determine probe-derived
133 (on-target) reads. The two probe sets yielded similar numbers of sequencing reads and mapped
134 reads (Fig. 2b). There was a larger variation in the proportion of uniquely mapped reads and
135 fewer on-target reads in the Allegro dataset compared to the JAX dataset, suggesting that the
136 JAX design pipeline may be more effective in selecting unique regions of each MAG. The
137 previously chosen 0.001% minimum probe-abundance and 10 probes per MAG (ppM)
138 thresholds were applied to the mouse samples (Fig. 2c). The number of MAGs observed in the
139 mouse samples after applying the thresholds decreased by ~50% (Fig. 2d). However, over 90%
140 of the reads matched MAGs present above the thresholds (Fig. 2d).

141 Comparison of the MAG abundances between the two designs without a probe
142 abundance threshold gave a Pearson correlation coefficient of 0.98, demonstrating that the
143 MAG abundance as measured by the Allegro and JAX probe sets were highly consistent (Fig.
144 3a). The points on the plot are colored by the number of probes detected in each MAG in both
145 probe sets, showing higher abundance and better concordance between the probe sets for
146 MAGs with reads from 10 or more probes. The MAGs were also plotted based on the number of
147 probes detected in each dataset across all mouse samples, illustrating that MAGs tend to have
148 high or low probe representation in both probe sets (Fig. 3b).

149

150 *Comparison of the MA-GenTA assay to other microbial community profiling assays*

151 mWGS data was available for 69 mouse fecal samples, enabling correlation of relative
152 abundance data for each MAG between the two assays. MAGs were separated into groups
153 based on the number of probes observed by MA-GenTA in each sample (e.g. from 1 to 20) and
154 a Pearson correlation was performed on each group of MAGs between the MA-GenTA and
155 mWGS abundance data (Fig. 3c and Supplementary Fig. 2, 3, Supplementary Table 2). For both
156 the Allegro and JAX datasets, MAGs with ≥ 15 probes detected have relative abundance
157 correlations of $R \geq 0.9$ to the mWGS data. MAGs represented by less than 10 probes had poor
158 Pearson correlations between the relative abundance of MA-GenTA and mWGS data ($R \leq 0.23$
159 for Allegro and $R \leq 0.52$ for JAX). Poor correlation of MAGs with fewer probes could be due to
160 poor probe performance, improperly assembled MAGs, pan-genome differences between the
161 MAG and the organisms present in our samples, sequencing depth disparities between the MA-
162 GenTA assay and mWGS, or inflated abundance values in mWGS caused by read-mapping
163 hotspots or conserved regions.

164 16S rRNA gene sequencing, mWGS, and the MA-GenTA assay are distinct ways of
165 determining the number of bacterial species present in a sample. We compared the number of
166 observed MAGs from the MA-GenTA assay with the number of 16S rRNA v1-v3 OTUs and MAGs
167 detected in the mWGS data across the mouse samples from three studies (Fig. 3d-g). A MAG
168 was considered present if at least 10 probes had $>0.001\%$ probe abundance. These thresholds
169 were used in subsequent analyses of mouse stool datasets. The sensitivity to detect a MAG
170 depends upon sequencing depth (more reads means it is more likely reads from a low-
171 abundance genome will be detected) and probe representation (if a MAG truly represents the
172 genome of a species present in the sample, then reads from a large fraction of probes should
173 be observed).

174 All the datasets were filtered with MAG/OTU relative abundance thresholds of 0.1%,
175 0.01%, 0.001%, and no threshold. The total number of MAGs across the all HLB samples was
176 compared between the MA-GenTA (JAX and Allegro) assay and mWGS at each threshold (Fig.
177 3d). There was a steep increase in the number of mWGS MAGs as thresholds were lowered,
178 while the MAGs in the JAX and Allegro assays increased slightly. The Venn diagram for each
179 threshold shows high overlap of MAGs detected between JAX and Allegro MA-GenTA datasets,

180 with an increasing number of low-abundance MAGs detected only in the mWGS assay. Within
181 the HLB dataset, the Allegro and JAX MA-GenTA datasets yielded similar numbers of MAGs,
182 which were also similar to the number of 16S OTUs across all thresholds on a per-sample basis
183 (Fig. 3e). The mWGS data detected similar numbers of MAGs to the 16S and targeted data for
184 the 0.1% and 0.01% relative abundance thresholds, but much larger numbers at the 0.001%
185 cutoff and without an abundance threshold. This observation is consistent with data shown in
186 Supplementary Fig. 4 where many MAGs had $\geq 0.01\%$ relative abundance in the mWGS data
187 (yellow tones), but lower abundance and <10 probes per MAG in both MA-GenTA datasets. The
188 CCF dataset consisted of JAX, Allegro, and mWGS data (Fig. 3f). Similar patterns to the HLB data
189 were seen, except that more MAGs were observed in the mWGS data than the MA-GenTA
190 MAGs at a 0.01% threshold. Most CCF samples that had more MA-GenTA reads than mWGS
191 reads; when the reference database was extended to include lower completeness MAGs, fewer
192 hqMAGs were observed using mWGS reads, suggesting that non-specific mapping could explain
193 some of the discrepancy (Supplementary Fig.5). In the VNDR dataset, only 16S rRNA data was
194 available for comparison. For these samples, more MAGs were detected by the MA-GenTA than
195 16S OTUs at lower abundances (Fig. 3g).

196 In order to demonstrate the utility of the MA-GenTA assay in characterizing microbial
197 profiles in an experimental context, we used the MA-GenTA datasets for analysis of the HLB
198 samples. Prior results identified OTU differences between C57BL/6J mice and HLB444 mice,
199 which carry a mutation in the *Klf15* gene, on both a standard chow diet and after introduction
200 of a high-fat, high-sugar diet (HF)²¹. HLB444 mice are resistant to diet-induced obesity when fed
201 the HF diet. To determine the ability of the MA-GenTA assay to differentiate these groups, the
202 Bray-Curtis dissimilarity metric was applied to the 16S, mWGS, and MA-GenTA data of the same
203 samples and viewed with non-metric multi-dimensional scaling (NMDS) plots (Fig. 4a). All assays
204 showed samples clustered by diet (Chow vs. HF) and mouse strain (C57BL/6J vs. HLB444).
205 PERMANOVA analysis for each of the sequencing assays confirmed significant clustering
206 between mouse strain and diet: Allegro assay ($f = 2.6961$, $p = 0.0029$), JAX assay ($f = 13.629$, $p =$
207 0.0009), 16S ($f = 19.581$, $p = 0.0009$), mWGS ($f = 2.05$, $p = 0.0099$) (Supplementary Table 3).
208

209 *Functional analysis using MA-GenTA*

210 Given the relative abundance of MAGs in each sample, we inferred the functional
211 potential of each sample based on links of proteins encoded in each MAG to KEGG pathways.
212 MA-GenTA read counts for each MAG in the HLB samples were assigned to KEGG pathways on a
213 per-sample basis and then converted to relative abundance. Linear discriminant analysis in
214 LEfSe was used to determine differentially abundant pathways between the two mouse strains
215 and the two diets. The number of differentially abundant pathways varied across comparisons
216 (HLB444 vs. B6 on HF diet (53,60), HLB444 vs. B6 on Chow (66,63), Chow vs. HF in HLB444
217 (101,103), and Chow vs. HF in B6 (75,81)) for the Allegro and JAX datasets respectively
218 (Supplementary Table 4). Inter-assay KEGG pathway concordance was 82% for HLB444 vs. B6 on
219 HF, 72% for HLB444 vs. B6 on Chow, 96% for Chow vs. HF in HLB444, and 77% for Chow vs. HF
220 in B6. Consideration of the response of HLB444 and B6 strains to the HF diet showed
221 differences in carbohydrate metabolism between the two strains on the HF diet, with HLB444
222 animals having higher representation of glycolysis, TCA cycle, and oxidative phosphorylation,
223 and B6 animals with higher representation of pathways related to utilization of other sugars
224 (Fig. 4b, Supplementary Figs. 6-13). These and other differences distinguished the response to
225 HF diet of these two mouse strains and suggest microbial differences contribute to the ability of
226 HLB mice to adapt to the HF diet.

227

228 *Specificity of MA-GenTA in a complex microbial environment*

229 As an additional way to assess the specificity of probe targeting, both probe sets were
230 used to assay metagenomic DNA extracted from a human stool specimen, which serves as a
231 highly complex microbial sample with few organisms in common with mouse fecal bacteria
232 (Supplementary Fig. 14). While there are deep-branching similarities in the gut microbiota of
233 human and mouse, there are major differences at the genus and species level^{11,22,23}. There
234 were sixteen MAGs detected in the human stool sample using the same thresholds for
235 detection as used for the mouse samples (minimum of 10 probes per MAG at $\geq 0.001\%$ probe
236 abundance). The taxa associated with the detected MAGs have previously been found in human
237 stool samples²⁴⁻³⁰.

238

239 Discussion

240 As the field of microbial community profiling grows, the need for informative, cost-
241 effective, and streamlined assays of microbial composition becomes more important. Although
242 initially developed for genotyping applications, we have shown that by combining results from
243 multiple rigorously selected probes per genome, the Allegro Targeted Genotyping Assay can
244 produce accurate microbial relative abundance data across at least three orders of magnitude
245 dynamic range at a cost that is only moderately higher than 16S rRNA profiling. MA-GenTA
246 bridges the gap between 16S rRNA gene sequencing and mWGS, combining some of the
247 strengths of each approach (Table 2).

248 A hallmark and major motivation of mWGS sequencing is the ability to analyze
249 functional capability of the organisms in an environment. Strategies have been described to
250 predict function based on OTU composition³¹⁻³³, but they are strongly dependent on the
251 reference databases and perform poorly on datasets from non-human-associated microbes³⁴.
252 Because probe design for the MA-GenTA assay requires reference genomes, this approach does
253 not contribute to bacterial discovery. However, gene and pathway abundance data can be
254 inferred from MA-GenTA data by pairing read counts to pathways represented in the reference
255 genomes more directly than based on 16S rRNA sequences.

256 Capture-based targeted sequencing methods have been widely used for exome
257 sequencing and cancer mutation profiling^{17,18,35}, and represent a potential alternative approach
258 for microbiome profiling. Guitor, *et al.* recently described a method for highly multiplexed
259 detection of antibiotic resistance genes and bacteria that relies on biotinylated capture
260 probes^{36,37}. These probes and streptavidin bead capture kits are costly and require each
261 specimen to be processed separately, making library preparation laborious. By contrast, the
262 Allegro workflow involves pooling after a sample-specific tagging step and combination of pools
263 can yield up to 3072 uniquely barcoded libraries on a single sequencing run. Up to 100k probes
264 can be included in a single Allegro design. Unlike array-based platforms³⁸, it is straightforward
265 to alter the design of the MA-GenTA probe pool with each reagent order, allowing both the

266 refinement of the selected probes for each genome and the inclusion of additional content over
267 time.

268 The ability to synthesize probes based on user-defined parameters allows for broad or
269 targeted study of microbial communities, specific species or strains, genes of interest, antibiotic
270 resistance or virulence markers. Probe designs that focus on universal genes may be a good
271 choice for species tagging, while probes targeting variable regions could provide additional
272 information on pangenome variation. An important factor to consider when designing a probe
273 pool for MA-GenTA is the reference database from which probes are chosen, including how
274 representative the database is of organisms present in the sample. Across mouse mWGS
275 samples, only about 60% of reads matched the iMGMC hqMAGs, reinforcing the need for a
276 more robust reference for the mouse stool microbial community. Further optimization of the
277 MA-GenTA assay might involve adjusting the number of probes per genome and how
278 thresholds for probe abundance and probe representation are used to reduce noise and
279 increase confidence of MAG assignment. Although not examined here, the specificity of the
280 MA-GenTA assay would also be advantageous in specimens with high proportions of host
281 genomic DNA where mWGS analysis is inefficient. The MA-GenTA assay could also be adapted
282 to an RNAseq format for quantitative gene expression analysis.

283

284 **Methods**

285 **Probe design and filtering**

286 The “high quality” MAG set from the integrated Mouse Gut Metagenomic Catalog
287 (iMGMC) was accessed from GitHub (<https://github.com/tillrobin/iMGMC>). The hqMAG set
288 comprised 830 dereplicated genome equivalents predicted to be >90% complete and <5%
289 contaminated based on analysis by CheckM¹⁶. Two probe design strategies were used. For the
290 JAX design, the probe selection program CATCH³⁹ was run on each hqMAG separately to design
291 over 50,000 40-base probes per MAG. BLAST was used to match probes to Prokka-annotated
292 ORFs⁴⁰. Probes with BLAST matches shorter than 40 bp in length or less than 100% identity
293 were removed, followed by probes corresponding to genome regions on a pre-defined discard
294 list. Discard regions included annotations listed as tRNAs, ribosomal proteins, and with encoded

295 proteins with the term “repeat” or “hypothetical” in the name. Probes were required to have
296 between 45 and 65% G+C nucleotides. Probes with multiple matches within the hqMAG or to
297 more than one hqMAG were also excluded. Probes matching the single-copy MUSiCC gene list⁴¹
298 were flagged for probe selection. All resulting probes were sent to Tecan Genomics (Redwood
299 City, CA) where probe compatibility was assessed for probe pool production based on the
300 Allegro Targeted Genotyping protocol, and probe pools with 20 probes per MAG were
301 synthesized (JAX design), with 10 representing MUSiCC genes and 10 representing non-MUSiCC
302 genes. The iMGMC hqMAGs were also used by Tecan Genomics to create a second probe pool
303 (Allegro design) with 20 probes per MAG. There were 16 MAGs that did not pass probe-
304 synthesis filtering metrics for the JAX design but were present in the Allegro design. The final
305 probe pools contained 16,600 probes for the Allegro design and 16,280 probes for the JAX
306 design. Cross-reference between the hqMAG set and the ZymoBIOMICS Microbial Community
307 Standard was determined using BLAST alignment⁴², resulting in 3 MAGs matching genomes
308 from the ZymoBIOMICS genomes (*Escherichia coli*, *Enterococcus faecalis*, and *Pseudomonas*
309 *aeruginosa*).

310

311 **DNA Extraction of Mouse Stool Pellets and Controls**

312 Genomic DNA isolated from mouse stool pellets from several studies was used for
313 evaluation of the MA-GenTA assay (Table 2). All procedures used for animal husbandry and
314 collection of specimens were approved by the Jackson Laboratory Animal Care and Use
315 Committee and research was conducted in conformity with the *Public Health Service Policy on*
316 *Humane Care and Use of Laboratory Animals*. The HLB and VNDR study pellets and positive
317 controls (*E. coli*, ZymoBIOMICS Mock) were lysed using Qiagen PowerBead garnet tubes with 1
318 mL Qiagen InhibitEX buffer. The lysate was then processed with the QiaCube HT instrument
319 using a modified Qiagen QIAamp 96 DNA QIAcube HT protocol²¹ (Svenson). Each sample (a
320 single stool pellet, 10-60 mg total weight) was added to a Qiagen PowerBead 0.7 mm garnet
321 tube with 1 mL of QIAGEN InhibitEX buffer. All samples were incubated at 65°C for 10 minutes
322 followed by 95°C for 10 minutes. The samples were then mechanically lysed for 2 cycles of 30
323 seconds at 3,700 RPM on a QIAGEN Powerlyzer 24 Homogenizer, with a 1-minute rest period

324 between cycles. Samples were then centrifuged at 10,000 x g for 1 minute, and then 200 μ L of
325 this lysate was then mixed with AL Buffer (285 μ L) and Proteinase K (5 μ L). The lysate was
326 incubated for 10 minutes at 70°C and followed by an ice incubation for 5 minutes. 485 μ L of
327 lysate was transferred to a QiaCube HT instrument, where the lysate was combined with 200 μ L
328 of 100% Ethanol and then bound to the Qiaamp 96 plate. Each well of the Qiaamp 96 plate was
329 then washed with 600 μ L of AW1 Buffer, AW2 Buffer, and then 100% Ethanol. DNA was then
330 eluted with 100 μ L of AE Buffer without using TopElute fluid. The CCF stool pellets were
331 homogenized with 500 μ L Tissue and cell lysis buffer (Lucigen[®]) by pipetting up and down. An
332 aliquot of 100 μ L was removed and treated with an enzyme cocktail (5 μ L 10 mg/mL lysozyme,
333 1 μ L lysostaphin (5000 U/mL), 1 μ L mutanolysin (5000 U/mL) and 20 μ L Tissue and cell lysis
334 buffer) for 30 minutes at 37°C. Buffer ASL (QIAGEN[®]) (200 μ L with 0.5 μ L anti-foaming agent
335 DX) was added to each tube and mixed. Samples were placed on a QIAGEN[®] TissueLyser II bead
336 beater for 2x 3 minutes (30 Hz) and then spun down in a microcentrifuge. Each sample (200 μ L)
337 was further processed on the QIAGEN QIAamp 96 DNA QIAcube HT protocol.

338

339 **Allegro Targeted Genotyping Sample Prep and Sequencing**

340 The Allegro Targeted Genotyping V2 protocol (publication number M01501, Tecan
341 Genomics, Inc.) was followed for library preparation of all samples in duplicate with the Allegro
342 and JAX probe pools. Briefly, gDNA samples were enzymatically fragmented, followed by
343 ligation of barcoded adaptors. Barcoded samples were then purified and pooled together in
344 groups of 48. Each pool of 48 samples was placed in an overnight annealing and extension
345 reaction with the probe pool, followed by an AMPure XP bead purification. A qPCR step was
346 used to determine the number of cycles used in the library amplification (18 cycles). Amplified
347 libraries were bead purified (AMPure XP) and pooled in equimolar ratios for sequencing. A no
348 template control (NTC), *Escherichia coli* gDNA (ATCC[®] 8739™), a human stool metagenome DNA
349 sample⁴³ (Petersen et al), and a defined composition microbial community control
350 (ZymoBIOMICS Microbial Community Standard, Cat # D6300) were used as controls. Libraries
351 created from the Allegro Targeted Genotyping Assay were pooled and sequenced on an
352 Illumina NovaSeq SP 2x150bp run, using the custom R1 primer and 1% spike-in of phiX174

353 library as recommended. Libraries were loaded on the NovaSeq SP at 60% of standard loading
354 per Allegro Targeted Genotyping Assay recommendation; only forward read data was used for
355 analysis.

356

357 **Data analysis**

358 *mWGS read mapping and 16S OTU generation*

359 The raw mWGS sequences were trimmed of adapters and low-quality bases using
360 Cutadapt version 1.14⁴⁴. Host contaminant sequences were identified and filtered out using
361 Kraken2 version 2.0.8-beta⁴⁵. The clean sequences were aligned against the reference (iMGMC
362 MAGs) using BWA version 0.7.12⁴⁶ with parameter settings: `bwa mem -M -P`. The non-primary
363 alignment reads were then filtered out using SAMtools version 0.1.19⁴⁷ with parameter setting:
364 `-F 256`. Reads were filtered using 97.5% ID and 50% coverage thresholds. Finally, the read count
365 table by bin for each sample was generated from the alignment file. On average, about 60% of
366 total mWGS reads mapped to the iMGMC 830 hqMAGs. 16S OTUs were generated for the HLB
367 and VNDR data with USEARCH, using previously published parameters^{21,48}.

368

369 *MA-GenTA read mapping and data analysis*

370 Raw sequences were trimmed using TrimGalore/CutAdapt to remove the 40 bp probe
371 (<https://github.com/FelixKrueger/TrimGalore>)⁴⁴. Read mapping to hqMAGs was performed
372 using BWA. Sequences of up to 110 bp downstream of the probes were mapped to the iMGMC
373 reference index. Reads mapped with <95.5% identity and $\leq 50\%$ query length were removed.
374 Secondary alignments with lower alignment scores were removed and then reads mapped to
375 multiple sites with similar alignment scores were removed, which resulted in uniquely mapped
376 reads. BEDtools intersect command was used to match read alignment locations to the genome
377 locations of the designed probes to provide “on-target” read counts, removing reads that
378 aligned to regions outside of the expected probe annealing location⁴⁹. Counts tables were
379 created representing the on-target read count and relative abundance of each probe in each
380 hqMAG and the summed read counts and relative abundance for all probes per hqMAG. All
381 analyses were performed in R (version 4.0.2)⁵⁰. Allegro and JAX designs were compared based

382 on the relative abundance per MAG and the number of probes per MAG matched in each
383 sample. A Pearson correlation was performed on the MAG abundance comparison between the
384 two designs and between each design and the relative abundance based on mWGS sequencing.
385 The JAX and Allegro data were compared to 16S and mWGS data for the same samples on the
386 basis of alpha (observed) and beta diversity (Bray-Curtis dissimilarity) metrics using Phyloseq⁵¹.

387 388 *Functional analysis*

389 Protein coding sequences in the hqMAGs were predicted using Prodigal⁵², implemented
390 in Prokka⁴⁰. Functional annotation of the predicted CDS regions was performed using EggNOG-
391 Mapper⁵³, using Diamond⁵⁴ for searches, and with overlap parameters requiring at least 25%
392 query and reference coverage. For each sample, the number of reads mapping to each MAG
393 was assigned to each KEGG pathway⁵⁵ for all constituent CDS regions. Differences in pathway
394 abundance among sample groups was determined using linear discriminant analysis effect size
395 with LEfSe⁵⁶.

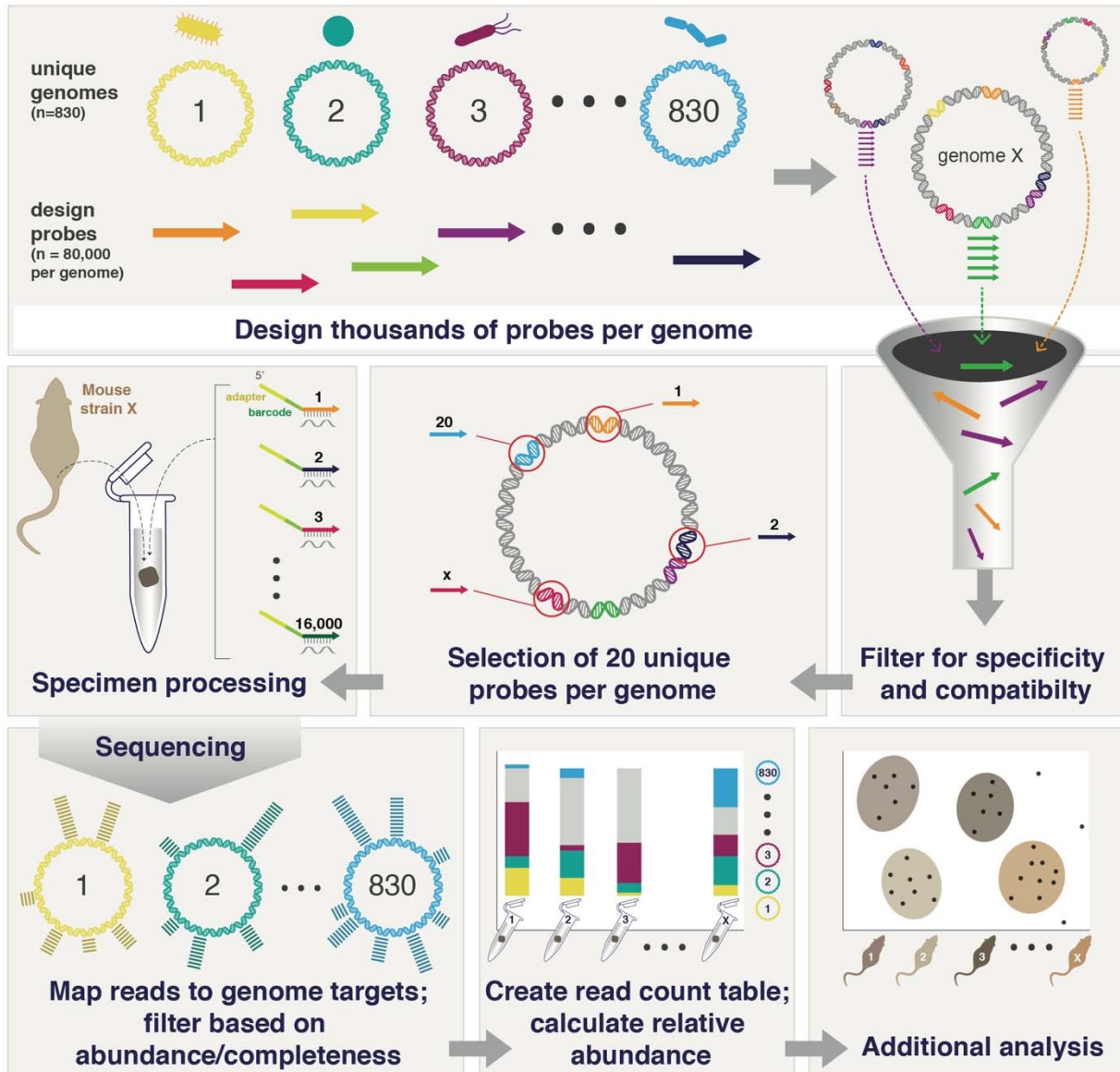
396 397 *Data Availability*

398 Sequence data created in this study have been deposited in GenBank with the
399 BioProject accession PRJNA646241. The probe sequences used for this study have been
400 deposited to GitHub: <https://github.com/TheJacksonLaboratory/MA-GenTA>.

401 *Code Availability*

402 All code used for probe design and data analysis, along with read count tables have
403 been deposited to GitHub: <https://github.com/TheJacksonLaboratory/MA-GenTA>.

404
405 **Acknowledgements:** We gratefully acknowledge the contribution of the Microbial Genomics
406 Service and Genome Technologies Service at The Jackson Laboratory for expert assistance
407 with the work described in this publication. We also gratefully acknowledge the Bioinformatics
408 team at Tecan Genomics for their assistance in probe pool design and analysis development.
409 We thank Julia Oh and John Graham for pre-publication access to mWGS data from stool
410 specimens of collaborative cross founder (CCF) mouse strains.

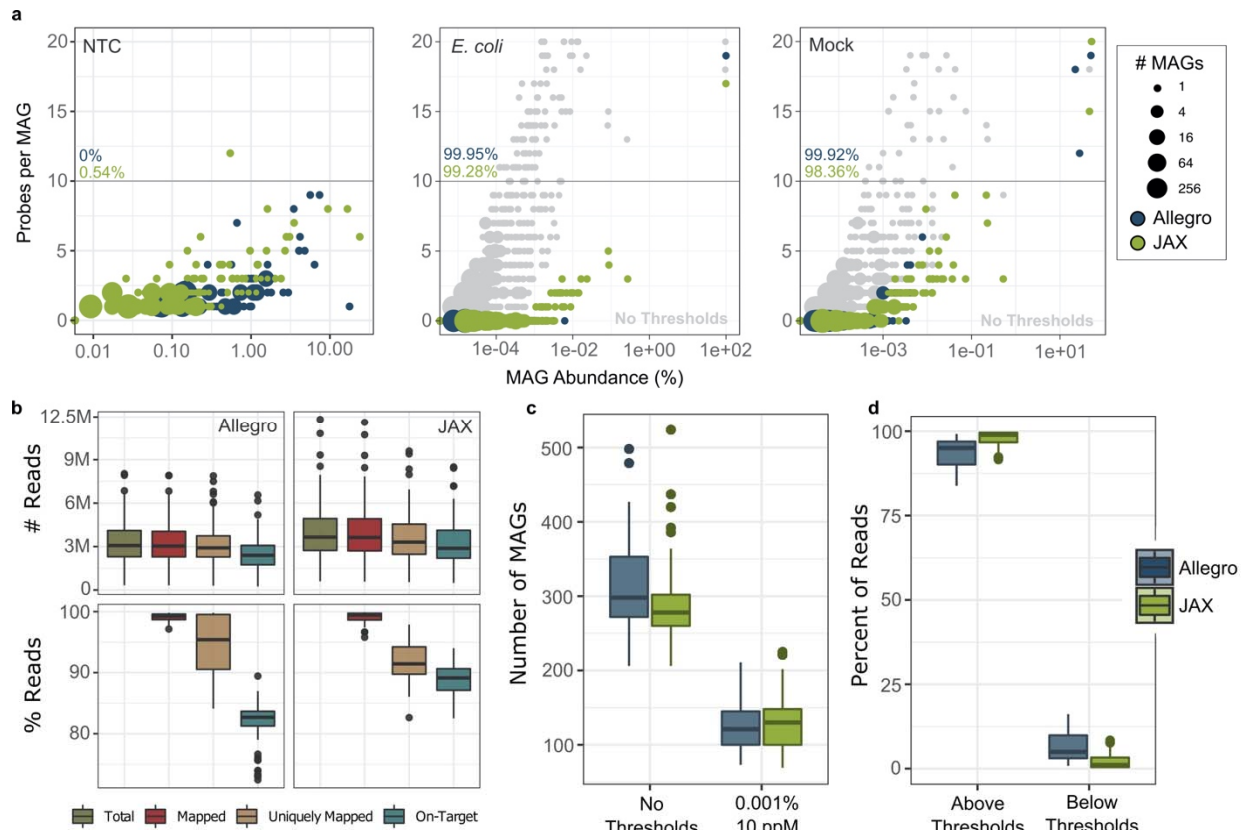


411

412 **Figure 1. Overview of the MA-GenTA strategy.** MA-GenTA utilizes software (CATCH) to design
413 thousands of probes per genome for multiple genomes (830 in this study). All probes from the
414 initial design are filtered based on multiple parameters (%GC, BLAST matches to
415 inclusion/exclusion lists, non-unique matches across genomes, etc). Unique probes are selected
416 for each genome (20 in this study). Probe pools are synthesized and used to prepare
417 sequencing libraries using the Allegro Targeted Genotyping kit, and then sequenced. Reads are
418 then mapped to the reference genomes to produce count tables for downstream analysis.

419

420

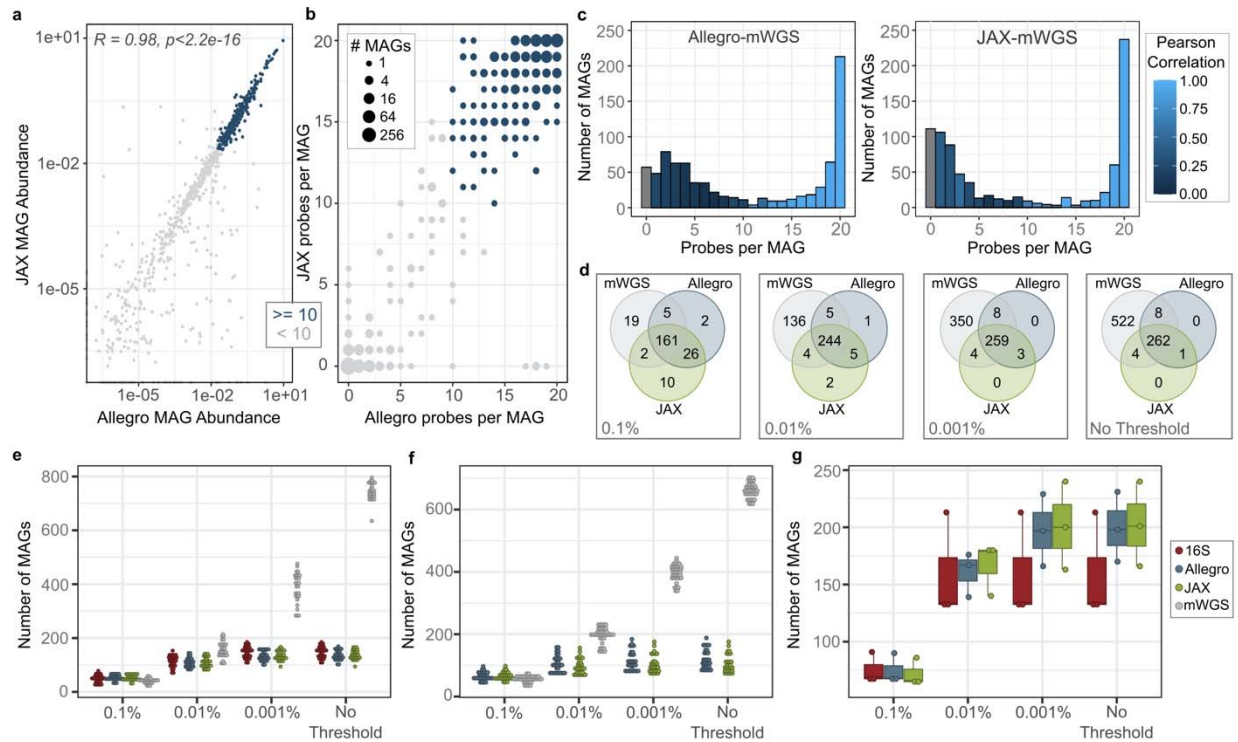


421

422 **Figure 2. Use of control samples to establish thresholds for defining MAG presence.**

423 Thresholds for declaring a MAG present in a sample were determined using a no template
 424 control (NTC), *Escherichia coli* genomic DNA, and ZymoBIOMICS Microbial Community
 425 Standard. **a**, The number of probes present for each MAG (y-axis) and the MAG abundance (x-
 426 axis) for each control sample before applied thresholds is shown in gray. Blue (Allegro) and
 427 green (JAX) points indicate MAGs detected in each control sample after a 0.001% minimum
 428 probe-abundance threshold was applied. **b**, Sequencing reads from the Allegro and JAX probe
 429 pools were mapped to the iMGMC hqMAGs. **Top**: Read counts per sample for total reads,
 430 aligned reads, uniquely mapped reads, and uniquely-mapped, on-target reads. **Bottom**: Same
 431 data as in the top panel, but expressed as percent of total reads. **c**, The number of MAGs
 432 detected with minimum probe abundance and probe representation (probes per MAG-ppM)
 433 thresholds is shown compared to the number of MAGs detected with no thresholds across
 434 mouse samples. **d**, Most reads correspond to probes that pass the probe-representation
 435 thresholds.

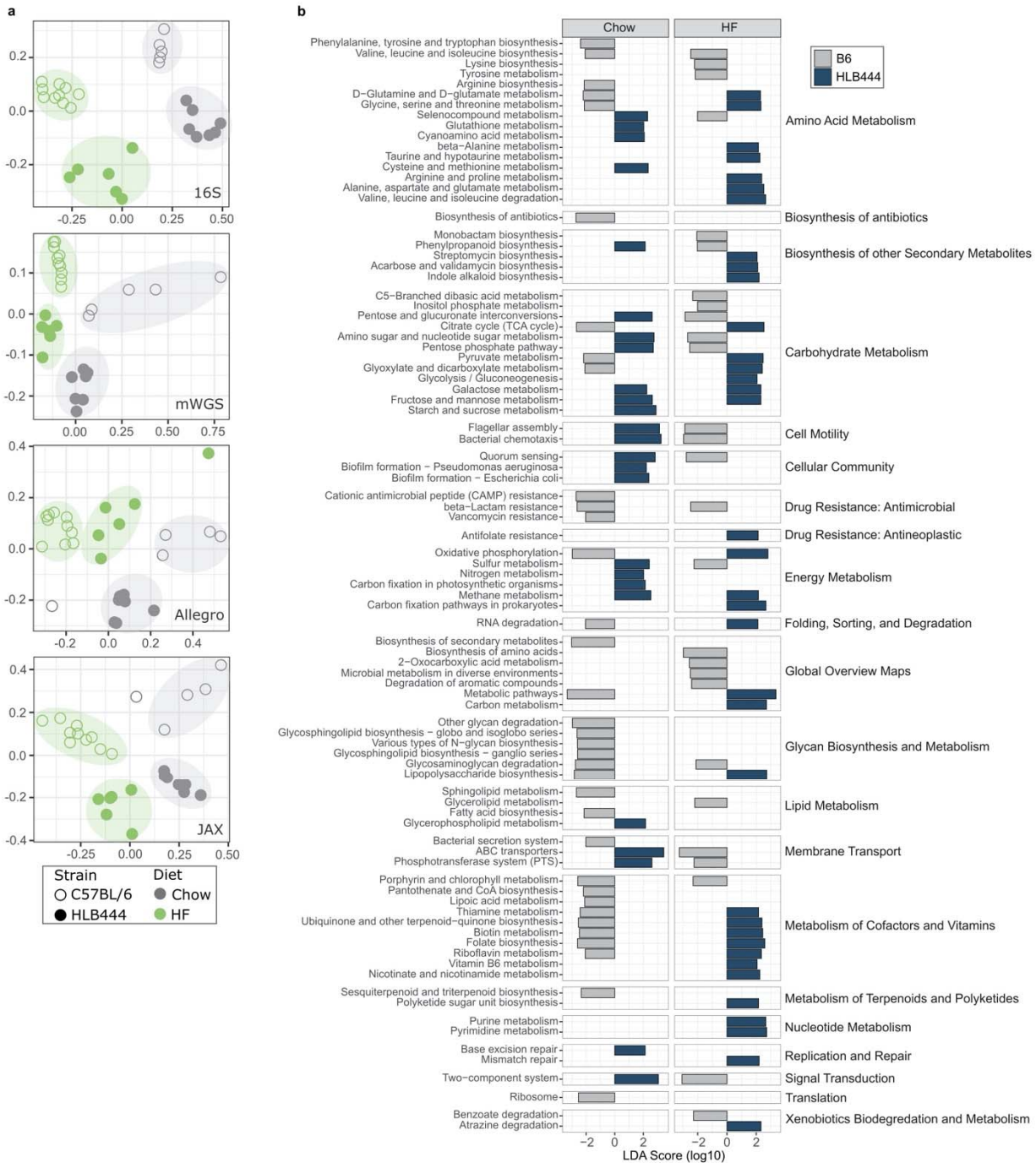
436



437

438 **Figure 3. Comparison of MA-GentA probe pools to established sequencing assays. a,** The
 439 percent relative abundance of each MAG in each sample based on the Allegro design (x-axis)
 440 and the JAX design (y-axis) is shown. MAGs with 10 or more probes above the 0.001% probe-
 441 abundance threshold in both designs are shown in blue. Pearson correlation of the two designs
 442 is $R = 0.98$. **b,** The number of probes per MAG detected using the Allegro design (x-axis) and JAX
 443 design (y-axis) As in C, MAGs with at least 10 probes with $\geq 0.001\%$ abundance in both assays
 444 are colored blue. Most MAGs have ≥ 15 probes per MAG above the threshold (top right) or ≤ 5
 445 (bottom left). **c,** The relative abundance of each MAG as inferred from the targeted and mWGS
 446 data was compared across the mouse stool samples using histograms showing the number of
 447 MAGs (y-axis) with the number of probes observed per MAG (x-axis) with no minimum probe-
 448 abundance threshold. The color-scale shows the Pearson correlation of the relative abundance
 449 between the Allegro (left) JAX (right) data and the mWGS data. **d,** The total number of MAGs
 450 present in each assay (JAX, Allegro, mWGS) are shown in Venn-diagrams, highlighting the
 451 overlapping MAGs between the assays. **e,** Samples from the HLB dataset are shown with 16S
 452 rRNA v1-v3 OTUs, and hqMAGs detected by Allegro, JAX, and mWGS assays at a range of
 453 minimum probe-abundance thresholds. **f,** CCF samples with hqMAGs detected by Allegro, JAX,

454 and mWGS assays. **g**, VNDR samples with 16S rRNA v1-v3 OTUs, and hqMAGs detected by
 455 Allegro and JAX assays.
 456



457
 458 **Figure 4. MA-GenTA as an assay for experimental group differentiation and functional**
 459 **analysis. a**, The Bray-Curtis dissimilarity metric was applied to HLB data from each sequencing

460 assay and shown in non-metric multi-dimensional scaling (NMDS) plots. Points are colored by
461 diet, closed circles represent HLB444 samples, and open circles are C57BL/6J samples. All four
462 sequencing assays cluster points based on diet and mouse strain. **b**, LDA analysis of KO
463 pathways inferred by MA-GenTA MAG abundances shows differentially abundant pathways
464 between HLB444 and B6 mouse strains on chow and HF diets.

465

466

467

468

469

470

471

472

473

474

475

476

477

478

479

480

481

482

483

484

485

486

487

488

489 Table 1. Mouse specimen groups used for analysis.

Study code	Summary	N samples	Data Type	Reference	BioProject Accession
HLB	C57BL/6J and HLB444 mice on chow and high-fat diet	29	16S	Svenson <i>et al.</i> ²¹	PRJNA505515
			mWGS	Unpublished	PRJNA646227
VNDR	C57BL/6J and C57BL/6N mice from three vendors	3	16S	Long, <i>et al.</i> , submitted for publication)	PRJNA622479
CCF	C57BL/6J, CAST, and PWK mice	40	mWGS	Oh, <i>et al.</i> , unpublished)	PRJNA646095

490

491

492 Table2. Comparison of microbial community profiling assays.

Feature	16S rRNA gene sequencing	Whole metagenome sequencing	MA-GenTA
Taxonomic Resolution	~Family/genus level for 16S rRNA subregions; strain level for full-length gene	Species/strain level	Species/strain level
Gene content	None	High	Inferred based on genome matches
Analysis complexity	Medium	High	Medium
Cost	<\$50/sample	>\$100/sample	\$50-\$75/sample
Pros	<ul style="list-style-type: none"> • Quick community survey • Large number of studies from many environments/hosts 	<ul style="list-style-type: none"> • New organism/gene discovery • Direct comparison of datasets with same reference for mapping 	<ul style="list-style-type: none"> • Efficient pooled-sample workflow • Customized target selection/pool composition • Direct comparison of datasets with same reference for mapping
Cons	<ul style="list-style-type: none"> • Limited taxonomic specificity • No gene content information 	<ul style="list-style-type: none"> • Possible mis-assignment of reads to closely related organisms • Cost 	<ul style="list-style-type: none"> • Limited to existing organisms/genomes • Limited pan-genome characterization

493

494

495

496 References:

- 497 1. Poretsky, R., Rodriguez-R, L. M., Luo, C., Tsementzi, D. & Konstantinidis, K. T. Strengths and
498 Limitations of 16S rRNA Gene Amplicon Sequencing in Revealing Temporal Microbial
499 Community Dynamics. *PLoS ONE* **9**, e93827 (2014).
- 500 2. Shin, J. *et al.* Analysis of the mouse gut microbiome using full-length 16S rRNA amplicon
501 sequencing. *Sci. Rep.* **6**, 29681 (2016).
- 502 3. Shoreline Biome. *Shoreline Biome* <https://www.shorelinebiome.com>.
- 503 4. Yang, B., Wang, Y. & Qian, P.-Y. Sensitivity and correlation of hypervariable regions in 16S
504 rRNA genes in phylogenetic analysis. *BMC Bioinformatics* **17**, 135 (2016).
- 505 5. Guo, F., Ju, F., Cai, L. & Zhang, T. Taxonomic Precision of Different Hypervariable Regions of
506 16S rRNA Gene and Annotation Methods for Functional Bacterial Groups in Biological
507 Wastewater Treatment. *PLOS ONE* **8**, e76185 (2013).
- 508 6. Johnson, J. S. *et al.* Evaluation of 16S rRNA gene sequencing for species and strain-level
509 microbiome analysis. *Nat. Commun.* **10**, 5029 (2019).
- 510 7. Ranjan, R., Rani, A., Metwally, A., McGee, H. S. & Perkins, D. L. Analysis of the microbiome:
511 Advantages if whole genome shotgun versus 16S amplicon sequencing. *Biochem. Biophys.*
512 *Res. Commun.* **469**, 967–977 (2016).
- 513 8. The Human Microbiome Project Consortium. A framework for human microbiome research.
514 *Nature* **486**, 215–221 (2012).
- 515 9. Ehrlich, S. D. MetaHIT: The European Union Project on Metagenomics of the Human
516 Intestinal Tract. *Metagenomics Hum. Body* 307–316 (2011).
- 517 10. Hugenholtz, F. & de Vos, W. M. Mouse models for human intestinal microbiota research: a
518 critical evaluation. *Cell. Mol. Life Sci.* **75**, 149–160 (2018).

- 519 11. Xiao, L. *et al.* A catalog of the mouse gut metagenome. *Nat. Biotechnol.* **33**, 1103–1108
520 (2015).
- 521 12. Parks, D. H. *et al.* Recovery of nearly 8,000 metagenome-assembled genomes substantially
522 expands the tree of life. *Nat. Microbiol.* **2**, 1533–1542 (2017).
- 523 13. Alneberg, J. *et al.* Genomes from uncultivated prokaryotes: a comparison of metagenome-
524 assembled and single-amplified genomes. *Microbiome* **6**, 173 (2018).
- 525 14. Almeida, A. *et al.* A unified catalog of 204,938 reference genomes from the human gut
526 microbiome. *Nat. Biotechnol.* 1–10 (2020).
- 527 15. Lesker, T. R. *et al.* An Integrated Metagenome Catalog Reveals New Insights into the Murine
528 Gut Microbiome. *Cell Rep.* **30**, 2909–2922.e6 (2020).
- 529 16. Parks, D. H., Imelfort, M., Skennerton, C. T., Hugenholtz, P. & Tyson, G. W. CheckM:
530 assessing the quality of microbial genomes recovered from isolates, single cells, and
531 metagenomes. *Genome Res.* **25**, 1043–1055 (2015).
- 532 17. Scaglione, D. *et al.* Single primer enrichment technology as a tool for massive genotyping: a
533 benchmark on black poplar and maize. *Ann. Bot.* **124**, 543–551 (2019).
- 534 18. Barchi, L. *et al.* Single Primer Enrichment Technology (SPET) for High-Throughput
535 Genotyping in Tomato and Eggplant Germplasm. *Front. Plant Sci.* **10**, (2019).
- 536 19. Bonde, M. T. *et al.* Direct Mutagenesis of Thousands of Genomic Targets Using Microarray-
537 Derived Oligonucleotides. *ACS Synth. Biol.* **4**, 17–22 (2015).
- 538 20. Hiatt, J. B., Pritchard, C. C., Salipante, S. J., O’Roak, B. J. & Shendure, J. Single molecule
539 molecular inversion probes for targeted, high-accuracy detection of low-frequency
540 variation. *Genome Res.* **23**, 843–854 (2013).

- 541 21. Svenson, K. L., Long, L. L., Ciciotte, S. L. & Adams, M. D. A mutation in mouse Krüppel-like
542 factor 15 alters the gut microbiome and response to obesogenic diet. *PLoS ONE* **14**, (2019).
- 543 22. Ley, R. E. *et al.* Obesity alters gut microbial ecology. *Proc. Natl. Acad. Sci.* **102**, 11070–11075
544 (2005).
- 545 23. Nguyen, T. L. A., Vieira-Silva, S., Liston, A. & Raes, J. How informative is the mouse for
546 human gut microbiota research? *Dis. Model. Mech.* **8**, 1–16 (2015).
- 547 24. Martínez, I., Muller, C. E. & Walter, J. Long-Term Temporal Analysis of the Human Fecal
548 Microbiota Revealed a Stable Core of Dominant Bacterial Species. *PLoS ONE* **8**, e69621
549 (2013).
- 550 25. Ormerod, K. L. *et al.* Genomic characterization of the uncultured Bacteroidales family S24-7
551 inhabiting the guts of homeothermic animals. *Microbiome* **4**, 36 (2016).
- 552 26. Johnson, J. L., Moore, W. E. C. & Moore, L. V. H. *Bacteroides caccae* sp. nov., *Bacteroides*
553 *merdae* sp. nov., and *Bacteroides stercoris* sp. nov. Isolated from Human Feces. *Int. J. Syst.*
554 *Bacteriol.* **36**, 499–501 (1986).
- 555 27. ricaboni, D., Mailhe, M., Khelaifa, S., Raoult, D. & Million, M. *Romboutsia timonensis*, a new
556 species isolated from human gut. *New Microbes New Infect.* **12**, 6–7 (2016).
- 557 28. Tytgat, H. L. P. *et al.* Complete Genome Sequence of *Enterococcus faecium* Commensal
558 Isolate E1002. *Genome Announc.* **4**, (2016).
- 559 29. Feng, Z. *et al.* A human stool-derived *Bilophila wadsworthia* strain caused systemic
560 inflammation in specific-pathogen-free mice. *Gut Pathog.* **9**, 59 (2017).
- 561 30. Song, Y. *et al.* '*Bacteroides goldsteinii* sp. nov.' Isolated from Clinical Specimens of Human
562 Intestinal Origin. *J. Clin. Microbiol.* **43**, 4522–4527 (2005).

- 563 31. Langille, M. G. I. *et al.* Predictive functional profiling of microbial communities using 16S
564 rRNA marker gene sequences. *Nat. Biotechnol.* **31**, 814–821 (2013).
- 565 32. Aßhauer, K. P., Wemheuer, B., Daniel, R. & Meinicke, P. Tax4Fun: predicting functional
566 profiles from metagenomic 16S rRNA data. *Bioinformatics* **17**, 2882–2884 (2015).
- 567 33. Ward, T. *et al.* BugBase predicts organism-level microbiome phenotypes. *BioRxiv* (2017).
- 568 34. Sun, S., Jones, R. B. & Fodor, A. A. Inference-based accuracy of metagenome prediction
569 tools varies across sample types and functional categories. *Microbiome* **8**, 46 (2020).
- 570 35. Lonigro, R. J. *et al.* Detection of somatic copy number alterations in cancer using targeted
571 exome capture sequencing. *Neoplasia* **13**, 019–1025 (2011).
- 572 36. Guitor, A. K. *et al.* Capturing the Resistome: A Targeted Capture Method To Reveal
573 Antibiotic Resistance Determinants in Metagenomes. *Antimicrob. Agents Chemother.* **64**,
574 (2020).
- 575 37. Allicock, O. M. *et al.* BacCapSeq: a Platform for Diagnosis and Characterization of Bacterial
576 Infections. *mBio* **9**, (2018).
- 577 38. Heller, M. J. DNA Microarray Technology: Devices, Systems, and Applications. *Annu. Rev.*
578 *Biomed. Eng.* **4**, 129–153 (2002).
- 579 39. Metsky, H. C. *et al.* Capturing sequence diversity in metagenomes with comprehensive and
580 scalable probe design. *Nat. Biotechnol.* **37**, 160–168 (2019).
- 581 40. Seemann, T. Prokka: rapid prokaryotic genome annotation. *Bioinformatics* **30**, 2068–2069
582 (2014).

- 583 41. Manor, O. & Borenstein, E. MUSiCC: a marker genes based framework for metagenomic
584 normalization and accurate profiling of gene abundances in the microbiome. *Genome Biol.*
585 **16**, 53 (2015).
- 586 42. Altschul, S. F., Gish, W., Miller, W., Myers, E. W. & Lipman, D. J. Basic local alignment search
587 tool. *J. Mol. Biol.* **215**, 403–410 (1990).
- 588 43. Petersen, L. M. *et al.* Community characteristics of the gut microbiomes of competitive
589 cyclists. *Microbiome* **5**, 98 (2017).
- 590 44. Martin, M. Cutadapt removes adapter sequences from high-throughput sequencing reads.
591 *EMBnet.journal* **17**, 10–12 (2011).
- 592 45. Wood, D. E., Lu, J. & Langmead, B. Improved metagenomic analysis with Kraken 2. *Genome*
593 *Biol.* **20**, 257 (2019).
- 594 46. Li, H. & Durbin, R. Fast and accurate short read alignment with Burrows-Wheeler transform.
595 *Bioinformatics* **25**, 1754–1760 (2009).
- 596 47. Li, H. *et al.* The Sequence Alignment/Map format and SAMtools. *Bioinformatics* **25**, 2078–
597 2079 (2009).
- 598 48. Edgar, R. C. Search and clustering orders of magnitude faster than BLAST. *Bioinformatics* **26**,
599 2460–2461 (2010).
- 600 49. Quinlan, A. R. & Hall, I. M. BEDTools: a flexible suite of utilities for comparing genomic
601 features. *Bioinformatics* **26**, 841–842 (2010).
- 602 50. R Core Team. R: A language and environment for statistical computing. (2017).
- 603 51. McMurdie, P. J. & Holmes, S. phyloseq: An R Package for Reproducible Interactive Analysis
604 and Graphics of Microbiome Census Data. *PLOS ONE* **8**, (2013).

- 605 52. Hyatt, D. *et al.* Prodigal: prokaryotic gene recognition and translation initiation site
606 identification. *BMC Bioinformatics* **11**, 119 (2010).
- 607 53. Huerta-Cepas, J. *et al.* Fast Genome-Wide Functional Annotation through Orthology
608 Assignment by eggNOG-Mapper. *Mol. Biol. Evol.* **34**, 2115–2122 (2017).
- 609 54. Buchfink, B., Xie, C. & Huson, D. H. Fast and sensitive protein alignment using DIAMOND.
610 *Nat. Methods* **12**, 59–60 (2015).
- 611 55. Kanehisa, M. & Goto, S. KEGG: kyoto encyclopedia of genes and genomes. *Nucleic Acids*
612 *Res.* **28**, 27–30 (2000).
- 613 56. Segata, N. *et al.* Metagenomic biomarker discovery and explanation. *Genome Biol.* **12**, R60
614 (2011).
- 615